Since January 2020 Elsevier has created a COVID-19 resource centre with free information in English and Mandarin on the novel coronavirus COVID-19. The COVID-19 resource centre is hosted on Elsevier Connect, the company's public news and information website.

Atmospheric Pollution Research 13 (2022) 101419

Contents lists available at ScienceDirect

Atmospheric Pollution Research

journal homepage: www.elsevier.com/locate/apr

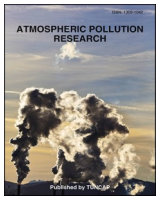

Association of population migration with air quality: Role of city attributes in China during COVID-19 pandemic (2019–2021)

Keyu Luo [a,1], Zhenyu Wang [a,*,1], Jiansheng Wu [a,b,**]

[a] Key Laboratory for Urban Habitat Environmental Science and Technology, School of Urban Planning and Design, Peking University, Shenzhen, 518055, PR China
[b] Key Laboratory for Earth Surface Processes, Ministry of Education, College of Urban and Environmental Sciences, Peking University, Beijing, 100871, PR China

ARTICLE INFO

Keywords:
Air quality
COVID-19
China
Migration
City attributes
Modification effects

ABSTRACT

Atmospheric pollution studies have linked diminished human activity during the COVID-19 pandemic to improve air quality. This study was conducted during January to March (2019–2021) in 332 cities in China to examine the association between population migration and air quality, and examined the role of three city attributes (pollution level, city scale, and lockdown status) in this effect. This study assessed six air pollutants, namely CO, NO_2, O_3, PM_{10}, $PM_{2.5}$, and SO_2, and measured meteorological data, with-in city migration (WCM) index, and inter-city migration (ICM) index. A linear mixed-effects model with an autoregressive distributed lag model was fitted to estimate the effect of the percent change in migration on air pollution, adjusting for potential confounding factors. In summary, lower migration was associated with decreased air pollution (other than O_3). Pollution change in susceptibility is more likely to occur in NO_2 decrease and O_3 increase, but unsusceptibility is more likely to occur in CO and SO_2, to city attributes from low migration. Cities that are less air polluted and population-dense may benefit more from decreasing PM_{10} and $PM_{2.5}$. The associations between population migration and air pollution were stronger in cities with stringent traffic restrictions than in cities with no lockdowns. Based on city attributes, an insignificant difference was observed between the effects of ICM and WCM on air pollution. Findings from this study may gain knowledge about the potential interaction between migration and city attributes, which may help decision-makers adopt air-quality policies with city-specific targets and paths to pursue similar air quality improvements for public health but at a much lower economic cost than lockdowns.

1. Introduction

In China, a country with a high level of air pollution (Aunan et al., 2018; Han et al., 2017), measures to control human activities have effectively improved air quality in recent decades. Although air pollution may be influenced by natural factors (Chen et al., 2020b; Zhang et al., 2020), the impact of human activities on air quality remains a topic of atmospheric pollution research. In the short term, special periods of control can bring about temporary improvements in air quality, such as the 2008 Olympics and the 2014 Asia-Pacific Economic Cooperation (APEC) meeting (Chen et al., 2013; Wang et al., 2016). In the medium-to long-term, relevant environmental policies may be powerful tools to reduce emissions and improve air quality (Xu and Zhang, 2020). The impact of these policies has been proved by a study that identified that pollutant reduction in China from 2013 to 2017 mainly came from a decline in anthropogenic emissions (Zhang et al., 2019).

COVID-19 has deeply impacted environmental quality in certain areas in the short term (He et al., 2021a; Zhao et al., 2021), because of

Abbreviations: AQI, air quality index; PRE, accumulated precipitation; PRS, atmospheric pressure; PRSR, range of atmospheric pressure; RHU, relative humidity; SSD, sunshine duration; TEM, temperature; TEMR, range of temperature; WIN, Wind speed; WCM, within-city migration; ICM, inter-city migration; SD, standard deviation; Skew, skewness; Kurt, kurtosis; F-test, variance ratio test; VIF, variance inflation factor; LSDV-ADL, a linear mixed-effects model with an autoregressive distributed lag.

Peer review under responsibility of Turkish National Committee for Air Pollution Research and Control.

* Corresponding author.
** Corresponding author.
E-mail addresses: zhenyu_wang@pku.edu.cn (Z. Wang), wujs@pkusz.edu.cn (J. Wu).

[1] Co-first author, these authors contributed equally to this work.

https://doi.org/10.1016/j.apr.2022.101419
Received 28 January 2022; Received in revised form 9 April 2022; Accepted 11 April 2022
Available online 18 April 2022

restrictions to limit exposure to the highly contagious virus (Bashir et al., 2020; Gautam, 2020; Rugani and Caro, 2020; Sharma et al., 2020). However, past air quality control studies have primarily focused on specific areas (Wang et al., 2021a). Methods based on large sample cities (including many small- and medium-sized cities) have rarely been examined. The impact of a decrease in comprehensive anthropogenic emission on air quality was more profound than that of previous local controls, providing a natural experiment between normal days and pandemic periods. Therefore, it would be helpful for us to explore the mechanism underlying different air pollutants' responses in various cities. However, city lockdown bans were highly inefficient to reduce pollution compared with other environmental regulations implemented in China. Similar levels of environmental welfare can be achieved at a much lower economic cost than lockdowns (Bherwani et al., 2020; Hu et al., 2021).

Traffic, industrial and residential sections were the major human emission sources in China (Aunan et al., 2018; Wang et al., 2021b). During the period of strict restrictions in response to COVID-19, China's air quality compliance rate increased by 36%, with NO_2 concentration decreased the most, indicating that control measures considerably reduced pollution emissions caused by the movement of people (Wang et al., 2020). The population migrations index may be considered as a proxy of human mobility affecting the emission sources during lockdown bans (Fang et al., 2020; Faridi et al., 2021). Indeed, the inter-city and intra-city traffic recorded a 37.8% and 14.0% drop, respectively, during the lockdown in Wuhan (Xiong et al., 2020). Consequently, the emission from traffic sources was reduced. Although the shutdown of certain industries (e.g. manufacturing and catering industries) contributed to the improved air quality (e.g., $PM_{2.5}$), almost no change in SO_2 concentration was observed in multiple cities because the production of certain steel, coking, gas, water, and power factories was not interrupted due to production needs (He et al., 2021b). In addition, pollution discharge from residential emissions (e.g., due to coal heating activities) and essential industry remained steady or not significantly declined (Faridi et al., 2021). Therefore, the pollution levels in cities with emissions dominated by coal power generation and residential sources were not significantly reduced (Kerimray et al., 2020).

Because there are obvious differences in climate, population distribution, economic structure, and urbanization process in Chinese regions with a vast territory (Wang et al., 2021a), air pollution variation during the lockdown also has regional characteristics. As shown in Table S1, only a few studies have identified larger lockdown effects in colder, richer, larger, more industrialized, and more air-polluted cities with previous heterogeneity analysis, suggesting interactions with city attributes (He et al., 2020; Hu et al., 2021; Shen et al., 2021; H. Wang et al., 2021a; Zeng and Bao, 2021). However, this cannot be deduced in all cases. Researches are insufficient for two reasons. First, previous studies have suggested the different modification effects based on zonal statistics but without causal inference (Naqvi et al., 2021). Approximately all studies have not quantified the city-specific marginal effect on air pollution decline due to migration during lockdown bans (Faridi et al., 2021). Zonal statistics may generate bias for mixing effect by lockdown measures with other confounding factors. It also faced the challenge to infer plausibly the average effect in each subclass of city attributes. Second, the directions of interactions are inconsistent with different pollution types and different modifiers. A study reported stronger PM or CO effects in cities with low green coverage rates, whereas it also reported weaker PM and SO_2 effects in cities with high vehicle density (Jia et al., 2021). The statistical significance of interaction also matters for detecting associations (Chen et al., 2018). To further empirically examine the intermediary modifier role of city attributes on air pollution decrease due to migration, to our knowledge, is a novel contribution.

Our study aimed to elucidate the modification effects of city attributes (i.e., pollution level, city scale, and response status) on the link between migration level and air quality. For example, the association between population migration and air pollution was expected to be stronger in cities that were polluted (versus clean), were large (versus small), or cities that adopted traffic restrictions (cities with versus no restrictions). This study utilized the daily observation data of migration (inter-city migration [ICM] and within-city migration [WCM]) and air pollution concentration ($PM_{2.5}$, PM_{10}, SO_2, CO, NO_2, and O_3) combined with meteorology factors and weekend dummy variables in 332 Chinese cities during January to March (2019–2020) using a linear mixed-effects model with an autoregressive distributed lag (LSDV-ADL). Our statistical methods have the advantage of reducing bias (due to confounding factors) compared with cross-sectional designs (Regencia et al., 2020). The large-sample analysis further helps address challenges from city-specific time-invariant characteristics and plausibly estimate the average effect in each subclass of city attributes (He et al., 2020). Our study has important policy-relevant implications. Our findings may gain knowledge about the potential interaction between migration and city attributes, which may support city-specific targets and paths for air pollution control. The modification effect of city attributes matters for employing initiatives by city managers and residents to reduce emissions, even at a relatively low level for public health. Future environmental policies should pursue similar air quality improvements likewise traffic restrictions but at a much lower economic cost.

2. Materials and methods

2.1. Sample and data

The research data covered 332 Chinese cities in January, February, and March (from 2019 to 2021). These three years were defined as the years before, during, and after the peak of COVID-19. This is also the annual period that spans the Chinese lunar new year, when there is large-scale migration with tens of millions of workers returning home and to their jobs. Thus, the date order was rearranged according to the lunar calendar, rather than the Gregorian calendar. Seventy-two days were selected for each year, from January 12 to March 24, 2019, from January 1 to March 12, 2020, and from January 19 to March 31, 2021, respectively. Time reorder benefited effective contemporaneous comparisons.

Population migration data were obtained from the Baidu migration service (http://qianxi.baidu.com/) using Python web crawler. Baidu is the most widely used Chinese search engine, equivalent to Google. The Baidu migration index was calculated based on the Baidu map user location, government database, and other cooperative third parties such as China mobile, which recorded multiple population migration types (Gibbs et al., 2020; Liu et al., 2020). The Baidu migration indices are unitless relative values that represent the spatial trajectory and characteristics of the population migration, and it does not distinguish between transport types. The dataset has been widely used in geo-economics, demography, and epidemiology, which has also served as an important data source for COVID-19-related research (Chen et al., 2020a; Gibbs et al., 2020).

Other data were also used in this study. Ground-observation air pollution data were collected from the online air quality monitoring and analysis platform of China (https://www.aqistudy.cn/). Daily meteorological data were obtained from the National Meteorological Science and Technology Data Center (http://data.cma.cn/). Population data were obtained from LandScan (satpalda.com/product/landscan/).

2.2. Measures of variables

The daily mean values of 699 ground reference stations were calculated using four automated observations. The air quality data included 332 cities with daily values throughout the study period. In the data-cleaning phase, outlier data were defined as empty values and extreme values. When the data were missing or there was no observation task, it was recorded as −9999 or 32,766. An extreme value is defined as the value of the measured values at each location that deviates from the

historical mean by more than 3 standard deviations). In general, the extreme values indicate that the actual measured value exceeds the upper and lower limits of the instrument, and a large value, such as 20,000 or 100,000, will be added to the original value when recording. These records were replaced with the average of nearby cities at a certain time. In addition, this study analyzed the descriptive statistics and correlation coefficients of the variables.

(1) Air-quality data

Air pollution data included the concentrations of PM_{10} ($\mu g/m^3$), $PM_{2.5}$ ($\mu g/m^3$), CO (mg/m^3), NO_2 ($\mu g/m^3$), 8-h average O_3 ($\mu g/m^3$), and SO_2 ($\mu g/m^3$) concentrations. All data were automatically updated hourly from the air monitoring stations. The daily concentrations in each city were averaged according to the hourly data of the day.

(2) Meteorological data

Air quality and pollution are largely related to the local meteorological conditions. Therefore, various meteorological factors were introduced as control variables to eliminate geographical and time differences. Eight meteorological factors were investigated, including atmospheric pressure of the station (PRS, hPa), range of atmospheric pressure (PRSR, hPa), precipitation (PRE, mm), average temperature (TEM, °C), range of temperature (TEMR, °C), average relative humidity (RHU, %), average wind speed (WIN, m/s), and sunshine duration (SSD, h). The arithmetic means at the city scale were obtained using geostatistics kriging interpolation and zonal statistics tools in ArcGIS 10.6. All data were projected onto the Krasovsky 1940 Albers coordinate system. The correlation within the data required further testing owing to the extensive meteorological indicators. A Pearson correlation coefficient >0.7 indicated a high correlation. In addition, the variance inflation factor (VIF) was used to test the severity of multiple collinearities in the multiple linear regression models. Data with a VIF >10 were excluded.

(3) Migration data

Traffic emission from migration is a key source of pollutants. The population migration data used in this study focused on the intensity of moving out of cities (MOC), the intensity of moving into cities (MIC), and the index of travel within cities (TIC). MOC and MIC, reflecting migration at the population scale, can be compared horizontally among different cities and years. TIC is the index of the ratio of the number of people traveling compared to the number of people living in the city. The urban migration boundary adopted an administrative division of the city, including districts, counties, townships, and villages. Population migration was estimated using previously described equations (Fang et al., 2020; Zeng and Bao, 2021) based on the proportional relationship between the Baidu migration index and population:

$$WCM = 2182.264 \times TIC \tag{1}$$

$$ICM = 90.848 \times (MOC + MIC) \tag{2}$$

where the WCM represents the within-city migration (1000 people), and ICM represents the inter-city migration (1000 people).

2.3. Models and data analysis procedure

(1) Spatio-temporal variation

Variations occurred in the air pollution and migration from 2019 to 2021. The city closure policy (lockdown) in Wuhan was initiated on January 23, 2020 (the 23rd day), and traffic control was gradually implemented in other cities. To compare the difference between the pollution concentrations before and after city closure with the same conditions over the same period in three consecutive years, the percentage change in the same period was calculated for each year. The change ratio between 2020 and 2019 reflected the impact of severe traffic control on population migration. The change ratio between 2021 and 2020 indicates the impact of the degree of migration recovery. The pollutant concentration curve plotted the average daily trend, whereas the confidence intervals represented the data dispersion.

Air pollution and migration factors were mapped at the national scale to show the spatial heterogeneity in the changes in both migrant and pollutant concentrations. The spatial autocorrelation and hot/cold spots of the variables were analyzed using the Local Moran's I index, which ranges from −1 to 1. A positive Moran's I value indicates that the $PM_{2.5}$ concentration presents a positive spatial autocorrelation, while a negative Moran's I indicates a negative spatial relationship. Based on the Euclidean distance, a spatial weight matrix with a normal distribution was established. The maximum K-nearest neighbor distance was used as the bandwidth. After 999 Mentcaro random permutations, a Moran's I p-value of Moran's I < 0.01 means the application of Moran's I is considered to be reliable. Otherwise, it would be considered unreliable. The ArcGIS 10.2 was used in this step.

(2) Statistical analysis

This study examined the modification effect by city attributes using a two-step stratified analysis. This research assumes that the association between pollutant concentrations and migration in cities with different attribute characteristics is different; that is, a modification effect of urban attributes exists. To estimate the stratified dataset, the regression model included air pollutants, time dummy variables, population migration, and meteorological data. If the coefficient p of the interaction term is significant, then the hypothesis holds.

First, an LSDV-ADL model was developed to estimate the association between each migration index and the percent change in air pollution. The least squares dummy variable method is a linear mixed-effects model with random subclass-specific intercepts. Mixed-effects models were fitted to account for the heterogeneity in each city's stratification. The autoregressive distributed lag model was employed to consider lagged items of air pollution because air pollutants can remain in the atmosphere for long durations. The study variables were endogenous and used as a function of the lagged values of the endogenous variables in the system, and the analysis was conducted using R software (version 3.6.2). The details of the LSDV-ADL model are as follows:

$$Air_{i,t} = \sum_{1}^{m} \alpha_r Class_r + \beta_1 lnICM_t + \beta_2 lnWCM_t + \beta_3 Weekend_t + \sum_{1}^{n} \gamma_p Weather_{p,t} + \sum_{1}^{q} \delta_q Air_{i,t-q} + u_t \tag{3}$$

where i, t, p, and q represent the pollution type, day, meteorological factor, and lagged days, respectively; $Air_{i,t}$ represents the i-th air pollution on day t; α_r of $Class_r$ denotes the fixed effect of each subclass; and ICM_t and WCM_t represent the inter-city migrants and within-city migrants on day t, respectively. To avoid the influence of non-stationary and heteroscedasticity, ICM and WCM were processed using a natural logarithm transformation. $Weather_{p,t}$ represents the p-th meteorological factor on day t; β, γ, and δ are the regression coefficients; α is the intercept; and u_t is the random error term. $Air_{i,t-q}$ represents the i-th air pollution lagged for q days before day t. Air pollutants' lifetimes in the atmosphere generally range from several days to one week; thus the moving average lag was used to estimate the lag effects (from lag 1 d to lag 7 d) of air pollutants. Weekend effects was also controlled, with 1 for the weekends and 0 for the weekdays. The concentrations of the six pollutants were used as the dependent variables. WCM and ICM are the independent variables, while the weekend dummy variable and

meteorological factors are control variables (confounding factors).

In the second step, city attributes (pollution level, city scale, and lockdown status) were assessed as effect modifiers using interaction terms. The quadruple division employed in this study investigates the modification effect of urban attributes in a robust manner, rather than the two- or three-category divisions used in most previous studies (Chen et al., 2018; Guo et al., 2021; Regencia et al., 2020). Stratifications of city attributes are shown in Fig. 1 and Table S2. First, the air pollution level was categorized according to the multi-year average AQI from 2015 to 2019 as good (<60), moderate (60–80), moderately polluted (80–100), and poor air quality (>100). Second, the city size was defined by population density (the ratio of population to area) ranked as small-sized (<100 people/km^2), medium-sized (100–500 people/km^2), large-sized (500–1000 people/km^2), and mega-sized (>1000 people/km^2) cities. Third, the subclass of lockdown response status included complete lockdown, partial lockdown (with-in city and inter-city), and no lockdown. Specifically, the complete lockdown cities experienced a mutation in both ICM and WCM, while the other lockdowns experienced only one. Mutations in the difference time series ΔICM and the ΔWCM between 2019 and 2020 were determined using the Mann–Kendall test. Combined with the stratified data, the interactions between air pollutants and city attribute dummy variables were added to the regression model. This was done to determine whether urban attribute factors significantly altered the relationship between air pollution and population migration.

3. Results

3.1. Air quality and population migration variables

Table 1 presents a summary of the variables, definitions, and descriptive statistics are presented in. The statistical results for the six

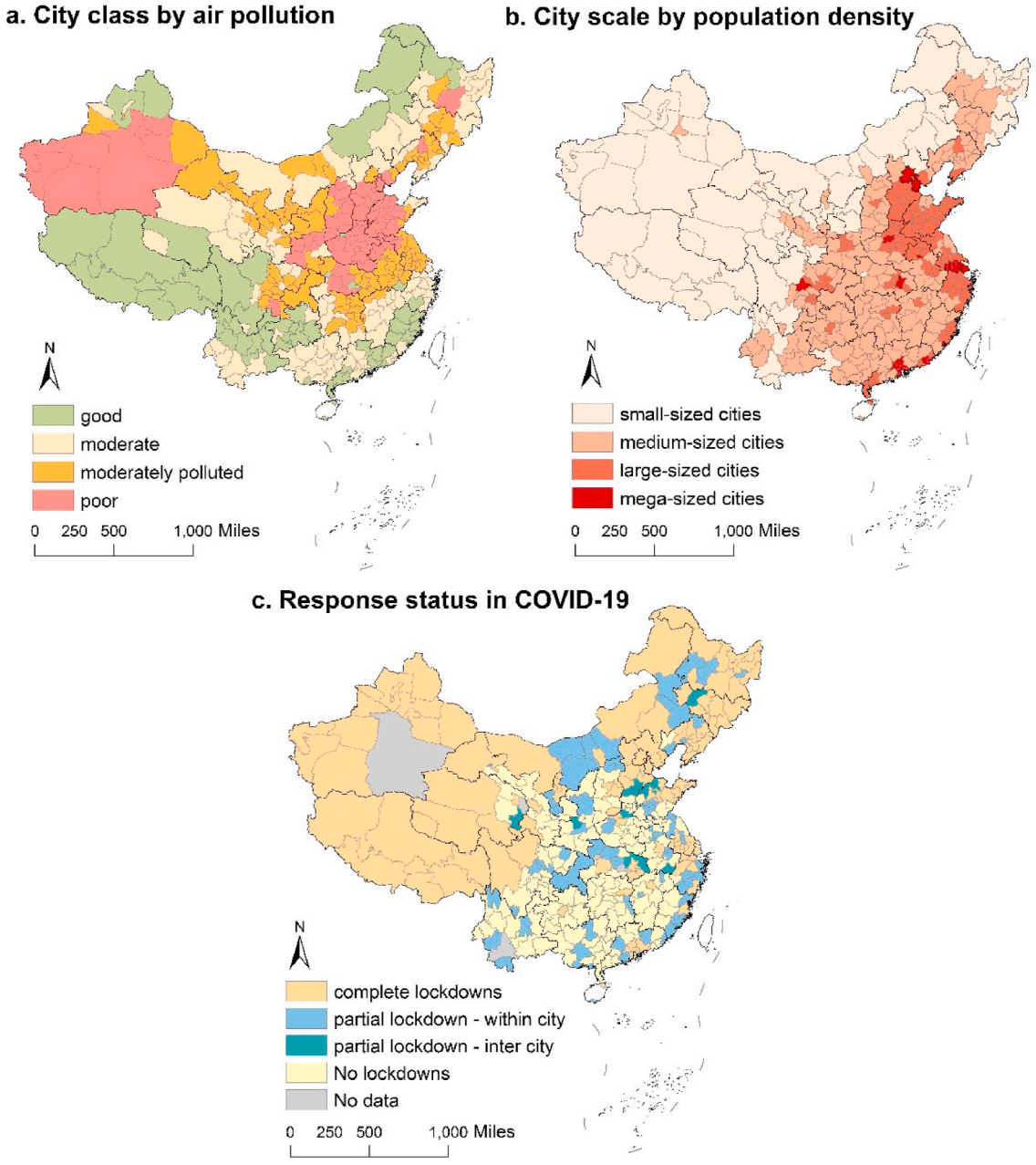

Fig. 1. City attributes stratifications and criteria: (a) air pollution subclass by average AQI; (b) city size subclass by population density; (c) subclass of lockdown response status.

Table 1
Summary of variables, definitions, and descriptive statistics (N = 71,712).

Variables	Variable definitions	Mean	SD	Min	Max	Skew	Kurt
Dependent variables: air pollution							
CO	CO concentration (mg/m^3)	0.90	0.45	0.10	7.40	2.54	9.33
NO_2	NO_2 concentration (μg/m^3)	27.32	16.06	1.00	145.00	1.09	1.37
O_3	8 h average O_3 concentration (μg/m^3)	75.63	26.96	2.00	300.00	0.13	0.42
PM_{10}	PM_{10} concentration (μg/m^3)	83.49	105.49	3.00	5058.00	15.91	469.49
$PM_{2.5}$	$PM_{2.5}$ concentration (μg/m^3)	50.05	42.51	1.00	1350.00	4.11	48.14
SO_2	SO_2 concentration (μg/m^3)	12.25	10.83	1.00	554.00	6.15	141.47
Independent variables: migration							
WCM	the number of within-city migrants (1000)	9823.42	2801.47	655.33	20955.41	−0.48	0.14
ICM	the number of inter-city migrants (1000)	170.63	228.50	0.26	3061.98	4.15	24.59
Control variables: meteorological data							
PRE	Accumulated precipitation	1.35	4.02	0.00	65.64	5.43	39.95
PRS	Atmospheric pressure	948.53	85.24	621.52	1034.59	−1.65	2.38
PRSR	Range of atmospheric pressure	5.74	2.32	1.07	65.31	2.15	15.21
RHU	Relative humidity	66.36	18.14	12.81	99.62	−0.40	−0.69
SSD	Sunshine duration	4.96	3.40	−3.24	14.30	−0.09	−1.39
TEM	Temperature	5.19	9.06	−39.48	29.59	−0.48	0.15
TEMR	Range of temperature	10.13	4.56	0.40	30.97	0.19	−0.73
WIN	Wind speed	2.25	0.81	−0.29	9.36	1.32	3.17
Weekend	Dummy variable, 1 for weekends, 0 for weekdays						

pollutant concentrations showed high pollutant variation. For example, $PM_{2.5}$ and PM_{10} far exceed the WHO thresholds of 25 μg/m^3 and 50 μg/m^3, with the largest standard deviation (SD) of 42.51 and 105.49 respectively. In addition, the Pearson correlation coefficients between ICM and WCM and other confounding variables were also <0.2. Pollution concentrations were strongly correlated, with the largest correlation coefficient between $PM_{2.5}$ and PM_{10} (0.73; Fig. S1 and Fig. S2). RHU (0.66), SSD (0.71), and TEMR (0.77) cannot coexist in the regression equation, because the information overlaps. Combined with the multicollinearity test in Table S3, PRS, RHU, TEMR, and WIN, with a VIF >10 were excluded from the candidate variables. By gradually removing these variables, the multicollinearity among the remaining variables was weakened (<7.5).

Furthermore, this study investigated whether the models were robust to different lag structures (Fig. S3). In general, the R^2 of the ADL model for different pollutants showed a similar trend, with a jump between

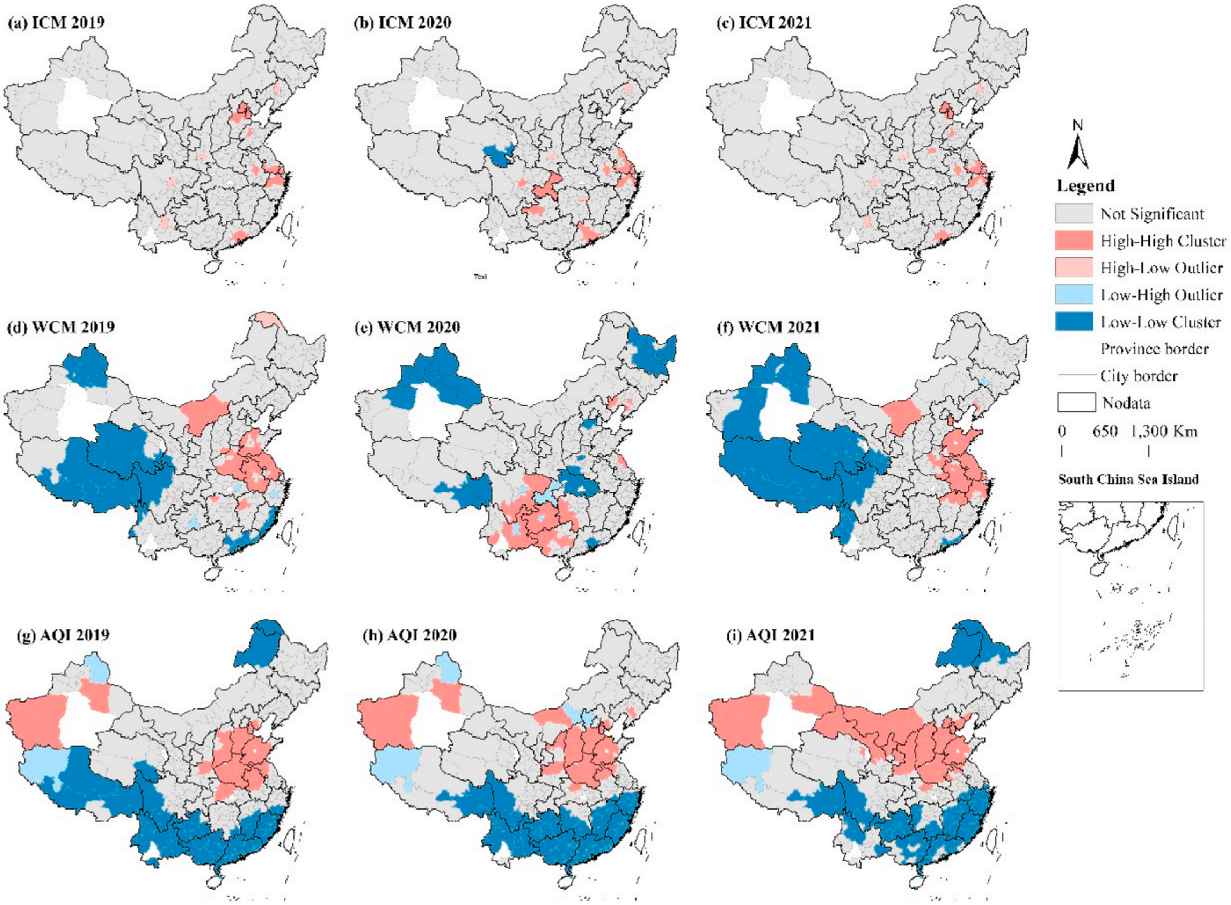

Fig. 2. LISA cluster mapper of population migration and AQI during the study period. Significant Local Moran's I ($p < 0.01$) is classified into four types: high-high, high-low, low-high, and low-low clusters.

lag0 and lag1. The optimal lag days for each pollutant were determined using the largest R^2 of ADL to improve the goodness of fit. Regression equations without the lag factor maintained the lowest goodness of fit, ranging from 0.0367 to 0.2712. The regression equation with the lag factors showed an initial increasing trend, followed by a decreasing trend after lag0. The optimal lag days in the ADL model for pollutants were inconsistent: $PM_{2.5}$ at lag1, PM_{10} at 1ag2, CO at lag6, SO_2 at lag5, NO_2 at lag4, and O_3 at lag4.

Air pollution data were obtained from the online air quality monitoring and analysis platform of China (https://www.aqistudy.cn/). Migration data were obtained from the Baidu migration website (http://qianxi.baidu.com/). Meteorological data were obtained from the National Meteorological Science and Technology Data Center (http://data.cma.cn/). The study duration was72 d in 2019, 2020, and 2021 (January 12, 2019–March 24, 2019; January 1, 2020–March 12, 2020; January 19, 2021–March 31, 2021). The data were then transferred and aggregated for the 332 cities. SD: standard deviation; Skew: skewness; Kurt: kurtosis.

3.2. Spatio-temporal change of migration and air pollution

(1) Changes in air pollution

The spatial distribution characteristics of AQI across China did not change significantly, with a high-high cluster in North China (Fig. 2). In 2019, the mean AQI of 18.67% of cities was >100, primarily in North China and southern Xinjiang. In 2020, the AQI of 48.4% of these cities decreased to <100, followed by a rebound in 2021. Figures S4 and S5 show the spatial distribution patterns of the six air pollutants (CO, NO_2, O_3, PM_{10}, $PM_{2.5}$, and SO_2). Moreover, the reason for the poor air quality in the northwest in 2021 lies in the PM_{10} sources (Fig. S7). A low $PM_{2.5}$/PM_{10} ratio (40–60%) shows that high pollution in North China in 2021 was mainly related to the northern transmission, with low humidity, sparse vegetation, and large desert areas in winter in the northwest.

The total air pollution concentrations changed dramatically in percentage during the three-year study period (Fig. 3d). The AQI in 2020 decreased by 7.1% from that in 2019 and increased by 8.8% in 2021. The CO, NO_2, SO_2, $PM_{2.5}$, and PM_{10} were reduced by 7.6%, 22.4%, 9.4%, 9.9%, and 19.13% in 2020 compared to 2019, respectively. In 2021, pollutants showed a year-on-year growth of 15.0% (CO), 1.7% (NO_2), 2.0% (SO_2), and 29.4% ($PM_{2.5}$) and 29.3% (PM_{10}). The lockdown start day as the inflection point of pollution trends is noticeable in Fig. 4 a–f. CO, NO_2, SO_2, $PM_{2.5}$, and PM_{10} generally showed a downward trend in 2020, while O_3 showed a reverse trend.

(2) Change of migration

Fig. 2 highlights the spatial autocorrelation of the ICM and WCM. High-high cluster areas of ICM were geographically located in large-scale urban agglomerations, while low-high cluster areas were located in

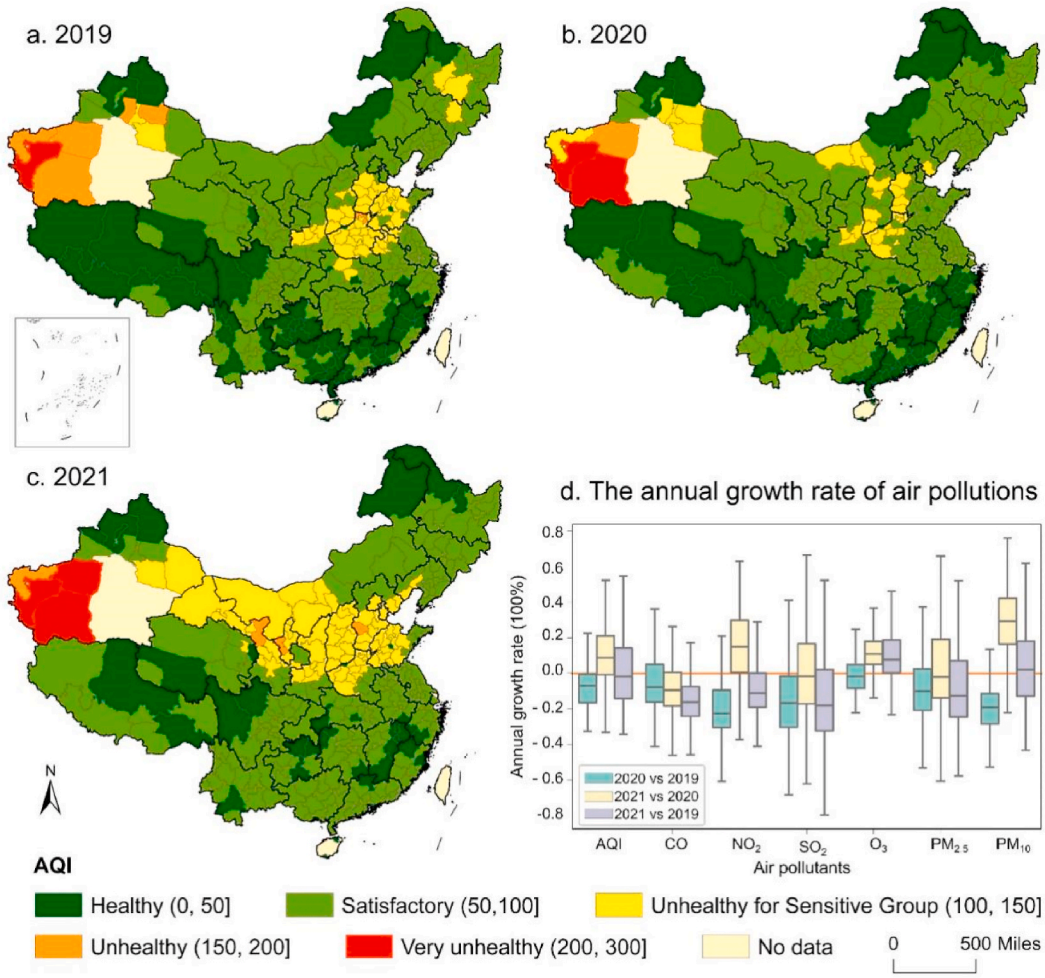

Fig. 3. Spatial-temporal variation in the degree of air pollution. Figures a–c map the air quality grade corresponding to the AQI mean values in 2019, 2020, and 2021. Figure d shows boxplots of the year-on-year growth rate of AQI and six air pollutants. The green boxes represent the change rates in 2019 with 2020, yellow boxes represent the change rates in 2020 with 2021, and purple boxes represent the change rates in 2021 with 2019. The orange line is y = 0.

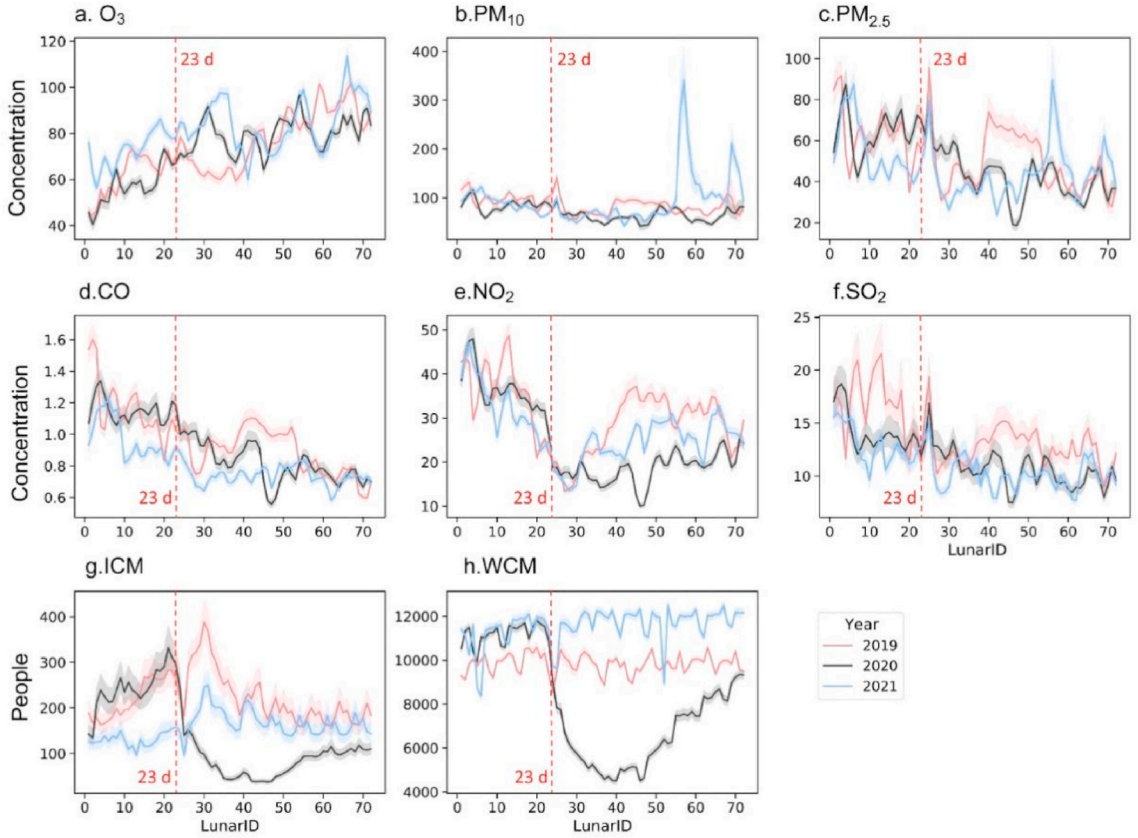

Fig. 4. Air pollution and migration curves of all cities in 2019, 2020, and 2021. The unit of CO is mg/m^3, and the unit of O_3 and PM_{10}, $PM_{2.5}$, NO_2, and SO_2 is μg/m^3. ICM and WCM represent population migration between cities and within cities (1000 people). Red, black and blue lines distinguish 2019, 2020, and 2021, respectively. The red dotted line marks day 23 when Wuhan, China went into lockdown.

the large cities or capital cities of various provinces. The high-high cluster areas of the WCM in 2020 transferred from north-central China to the southwest region. However, the pandemic situation across the country has not changed the spatial distribution characteristics of ICM across China.

High rates of change in migration also occurred in major urban agglomerations and provincial capitals (Fig. 5). When setting 23 d as the demarcation point of daily average ICM and WCM (Fig. 4 g–h), the average ICM and WCM in 2020 dropped significantly by 59.1% and 31.7%, respectively. When comparing 2021 with 2019, ICM dropped by an average of 24.25%, however, WCM increased by 19.9% on average; this is different from the overall migration decline in 2020 (Fig. 4 g–h and Fig. 5).

3.3. *Effect modification by city attributes*

(1) Effect modification by pollution level

Table 2 and Table 5 present the result of the effect modification by the pollution level. Pollution concentration was positively related to migration indices, other than O_3. In general, the air pollution modification effect strengthened the association of ICM with NO_2, but weakened the associations of ICM with O_3, PM10, $PM_{2.5,}$ and SO_2; while the air pollution modification effect strengthened the associations of WCM with NO_2, O_3, and PM_{10}.

Changes in NO_2 concentrations in cities with different pollution levels (good, 0.054 μg/m^3; moderate, 0.1093 μg/m^3; moderately polluted, 0.1081 μg/m^3; polluted, 0.1104 μg/m^3) were found an incremental associated with a 10% change in ICM. Similarly, the association between NO_2 and WCM was stronger in more-polluted (moderately polluted, 0.3491 μg/m^3; polluted, 0.3547 μg/m^3) versus less-polluted (good, 0.2103 μg/m^3; moderate, 0.3418 μg/m^3) cities.

The association between PM_{10} and WCM (a 10% change) was stronger in more-polluted (moderately, 1.9077 μg/m^3; poor, 2.8887 μg/m^3) versus less-polluted cities (good, 0.5517 μg/m^3; moderate, 1.1030 μg/m^3), however, no significate association was apparent with ICM ($p > 0.05$). Positive correlations were found between $PM_{2.5}$ and a 10% change in ICM (0.1693 μg/m^3), and WCM (0.3534 μg/m^3). Only a −0.0873 μg/m^3 modification effect of a 10% ICM change was found between cities with good and moderate air quality. The difference in the estimates of WCM among the cities was not statistically significant.

O_3 concentration was negatively correlated with migration. The effect of WCM on the 10% change in O_3 was also stronger for more-polluted cities (moderate, 0.3867 μg/m^3; moderately polluted, 0.4222 μg/m^3; poor, 0.5495 μg/m^3). However, the effect of ICM on O_3 was weaker in polluted (−0.0383 μg/m^3) versus less-polluted cities (−0.1533 μg/m^3). A generally positive association was estimated between SO_2 and an ICM change by 10% (0.021 μg/m^3), with a −0.0172 μg/m^3 modification effect in cities with moderate air quality compared with those with good air quality. A null association was found for the WCM-SO_2 relationship. This study also estimated a generally positive association between CO and an ICM change by 10% (1.1 μg/m^3), a null association for WCM and CO (1.4 μg/m^3, $p > 0.05$), and a null modification of different pollution levels to the migration-CO relationship.

(2) Effect modification by city scale

Table 3 and Table 5 present the results of effect modification by city scale. The city-scale modification effect strengthened the associations of WCM with NO_2 but weakened the associations of WCM with PM_{10} and $PM_{2.5}$, while the air pollution modification effect weakened the associations of ICM with $PM_{2.5}$.

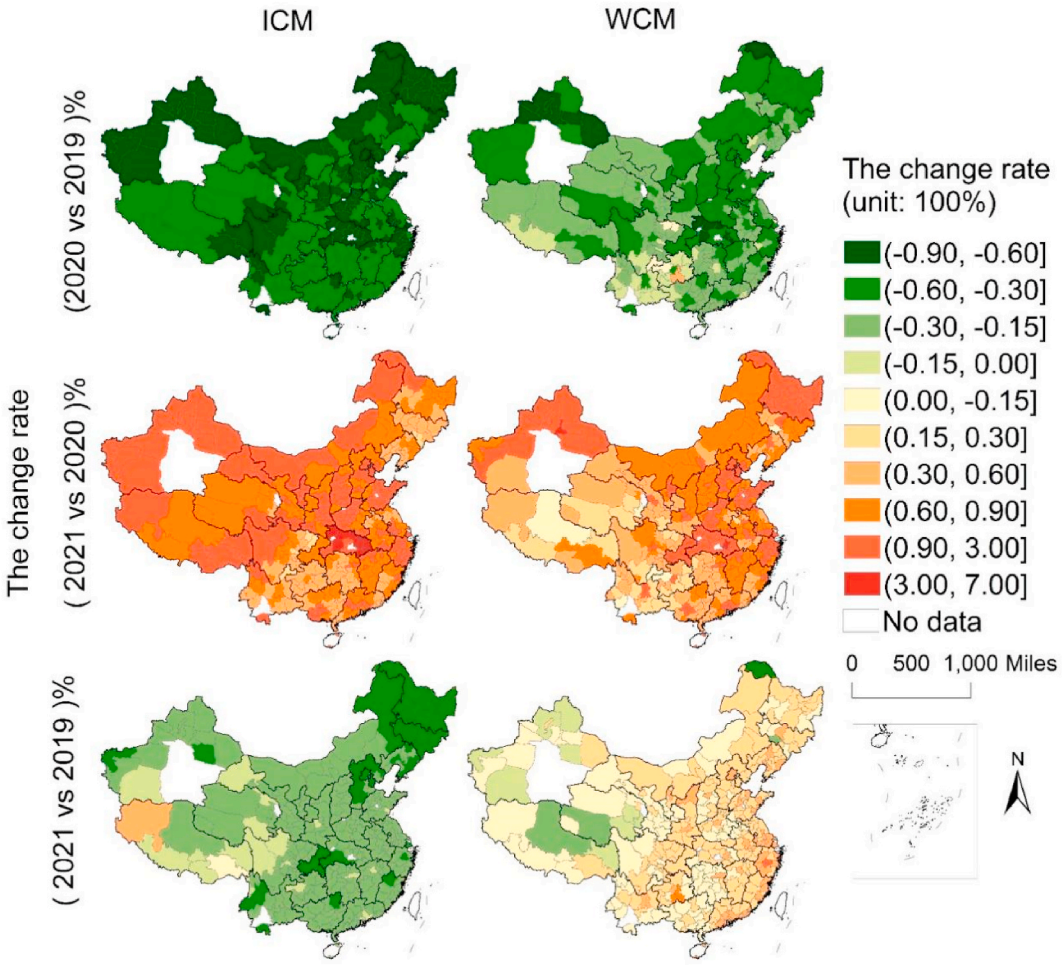

Fig. 5. Maps of the migration change rates. The unit of the change rate is 100%. There was a widespread decrease in migration across the country after January 23, 2020, while the number of migrants in 2021 climbed significantly over the same period when compared with 2019.

Table 2
Regression of city stratifications at different air pollution levels.

Coefficients	CO	NO_2	O_3	PM_{10}	$PM_{2.5}$	SO_2
Constant						
good	0.137 *	−15.093 ***	4.141	−39.701 ***	−13.911	−0.525
moderate	−0.085	−27.729 ***	39.618***	−72.148 ***	−13.043 *	−3.331 **
moderately polluted	0.156 **	−26.893 ***	42.133 ***	−120.442 ***	−6.766	−3.539 **
poor	0.157 **	−26.773 ***	51.482 ***	−164.801 ***	7.236	−3.304 *
Main effects						
ln*(ICM)*	0.011 ***	0.540 ***	−1.553 ***	0.793	1.693 ***	0.210 ***
ln*(WCM)*	0.014	2.103 ***	3.004 ***	5.517 *	3.534 ***	0.143
Weekends	−0.003	−0.144	1.133 ***	2.314 **	−0.327	0.000
Interaction effects						
ln*(ICM)*good*	reference	reference	reference	reference	reference	reference
ln*(ICM)*moderate*	0.005	0.553 ***	−0.050	−1.819 *	−0.873 **	−0.172 **
ln*(ICM)*moderately polluted*	−0.012 ***	0.541 ***	0.364	−4.812 ***	0.058	−0.404 ***
ln*(ICM)*poor*	−0.008 *	0.564 ***	1.170 ***	−10.670 ***	0.527	−0.097
ln*(WCM)*good*	reference	reference	reference	reference	reference	reference
ln*(WCM)*moderate*	0.024 *	1.315 ***	−3.867 ***	5.513	0.867	0.420
ln*(WCM)*moderately polluted*	0.008	1.388 ***	−4.222 ***	13.560 ***	0.375	0.574 *
ln*(WCM)*poor*	0.008	1.444 ***	−5.495 ***	23.370 ***	−0.281	0.402
R^2	0.921	0.908	0.943	0.624	0.785	0.823
F-statistic	32,685 ***	28,870 ***	48,738 ***	5427 ***	12,593 ***	12,431 ***

Note: Adjusted effect estimates of per 1% unit change in air pollution percentage change of ICM and WCM: single-pollution model with random subclass-specific intercept. Models for daily pollutant data (CO, NO_2, O_3, $PM_{2.5}$, PM_{10}, and SO_2) were adjusted for migration (WCM and ICM), meteorological factors (temperature, accumulated precipitation, wind speed, range of atmospheric pressure, and sunshine duration), and weekend effect (weekend and weekday), incorporating city subclass as the random effect. Significant codes: ***: p-value < 0.001; **: p-value < 0.01; *: p-value < 0.05.

Table 3
Regression of city stratifications at different scales.

Coefficients	CO	NO_2	O_3	PM_{10}	$PM_{2.5}$	SO_2
Constant						
small	0.198 **	−15.427 ***	25.599 ***	−182.419 ***	−36.653 ***	−4.316 ***
medium	−0.009	−23.113 ***	31.681 ***	−80.910 ***	−5.801	−4.411 ***
large	0.076	−39.223 ***	41.542 ***	−98.096 ***	−10.374	−1.245
mega	0.076	−45.771 ***	27.788 ***	−66.328 **	−4.826	0.571
Main effects						
ln*(ICM)*	0.012 ***	0.895 ***	−0.879 ***	−1.683	1.854 ***	0.087
ln*(WCM)*	0.006	2.043 ***	0.639	24.138 ***	6.146 ***	0.598 **
Weekends	−0.003	−0.058	1.178 ***	2.384 **	−0.136	0.012
Interaction effects						
ln*(ICM)*small*	reference	reference	reference	reference	reference	reference
ln*(ICM)*medium*	0.001	−0.368 **	−0.876 ***	1.187	−0.242	−0.152
ln*(ICM)*large*	−0.007	−0.314 ***	0.015	2.863 *	−0.708	−0.145
ln*(ICM)*mega*	−0.010	−0.010 ***	−0.814	1.181	−2.337 ***	−0.229
ln*(WCM)*small*	reference	reference	reference	reference	reference	reference
ln*(WCM)*medium*	0.025 *	1.149 ***	−0.508	−12.051 ***	−2.785 *	0.160
ln*(WCM)*large*	0.020 *	2.910 ***	−1.750 *	−10.147 **	−1.392	−0.193
ln*(WCM)*mega*	0.020	3.644 ***	0.316	−13.531 ***	−1.465	−0.360
R^2	0.921	0.907	0.943	0.616	0.777	0.823
F-statistic	32,543***	28,575***	48,760***	5254***	12,038***	12,441***

Note: Adjusted effect estimates of per 1% unit change in air pollution percentage change of ICM and WCM: single-pollution model with random subclass-specific intercept. Models for daily pollutant data (CO, NO_2, O_3, $PM_{2.5}$, PM10, and SO_2) were adjusted for migration (WCM and ICM), meteorological factors (temperature, accumulated precipitation, wind speed, range of atmospheric pressure, and sunshine duration), and weekend effect (weekend and weekday), incorporating city subclass as the random effect. Significant codes: ***: p-value < 0.001; **: p-value < 0.01; *: p-value < 0.05.

A 10% change in ICM was found an incremental associated with NO_2 concentration changes in cities of different scales (small, 0.2043 μg/m^3; medium, 0.3192 μg/m^3; large, 0.4953 μg/m^3; mega, 0.5687 μg/m^3). The modification effect of city scale on the 10% change in ICM to NO_2 could not be inferred (small, 0.0895 μg/m^3; medium, 0.0527 μg/m^3; large, 0.0581 μg/m^3; mega, 0.0885 μg/m^3).

A weakened modification effect of WCM to PM_{10} was found at the city scale, as the change in PM_{10} with a 10% change in WCM was greater in smaller (2.4138 μg/m^3) versus larger cities (medium, 1.2087 μg/m^3; large, 1.3991 μg/m^3; 1.0607 μg/m^3). In contrast, the differences between the estimates of ICM and PM_{10} among cities of various sizes were not statistically significant. The effect of the 10% change in ICM on $PM_{2.5}$ was weakened in larger (mega, −0.0483 μg/m^3; large: 0.1612 μg/m^3) versus smaller cities (small, 0.1854 μg/m^3; medium, 0.1146 μg/m^3). Similarly, the association of the 10% change in WCM on $PM_{2.5}$ was slightly weaker in larger (mega, 4681 μg/m^3; large, 0.4754 μg/m^3) versus smaller (small, 0.6146 μg/m^3; medium, 0.3361 μg/m^3) cities. City-scale modifications of the effect of migration (WCM and ICM) was not found on O_3, SO_2, and CO.

(3) Effect modification by response status

Table 4 and Table 5 present the results of effect modification by response status. The response status modification effect strengthened the associations between WCM-NO_2 and ICM-NO_2, but weakened the associations between ICM-$PM_{2.5}$.

A 10% change in ICM was associated with NO_2 concentration changes in cities with different response statusrd to COVID-19 (no, 0.0602 μg/m^3; inter, 0.1889 μg/m^3; intra, 0.0923 μg/m^3; complete, 0.1102 μg/m^3). Similarly, the association of 10% change in WCM with

Table 4
Regression analysis of city stratifications with different response status.

Coefficients	CO	NO_2	O_3	PM_{10}	$PM_{2.5}$	SO_2
Constant						
no	0.103	−23.257 ***	35.307 ***	−89.449 ***	11.824	−1.779
inter	0.315	−25.538 ***	49.205 ***	−28.974	55.986 **	−2.440
intra	−0.014	−30.912 ***	29.498 ***	−120.180 ***	−8.625	−4.132 **
complete	0.041	−30.484 ***	31.981 ***	−110.970 ***	−19.351 ***	−3.250 ***
Main effects						
ln*(ICM)*	0.024 ***	0.602 ***	−1.256 ***	0.432	4.104 ***	0.074
ln*(WCM)*	0.011	3.096 ***	−0.527	12.554 ***	0.091	0.375 *
Weekends	−0.004	−0.104	1.153 ***	2.382 **	−0.361	−0.003
Interaction effects						
ln*(ICM)*no*	reference	reference	reference	reference	reference	reference
ln*(ICM)*inter*	0.008	1.287***	0.067	7.720 ***	4.671 ***	0.150
ln*(ICM)*intra*	−0.017 ***	0.321 **	−0.144	−0.568	−2.128 ***	−0.113
ln*(ICM)*complete*	−0.016 ***	0.500 ***	0.356	−0.636	−1.356 ***	0.038
ln*(WCM)*no*	reference	reference	reference	reference	reference	reference
ln*(WCM)*inter*	−0.025	−0.294	−1.277	−9.390	−6.696 **	0.000
ln*(WCM)*intra*	0.021*	0.756 *	0.800	3.734	3.266 **	0.320
ln*(WCM)*complete*	0.016	0.705 *	0.402	3.248	4.026 ***	0.135
R^2	0.921	0.906	0.943	0.616	0.775	0.823
F-statistic	32,541***	28,489 ***	48,636 ***	5246 ***	11,919 ***	12,417 ***

Note: Adjusted effect estimates of per 1% unit change in air pollution percentage change of ICM and WCM: single-pollution model with random subclass-specific intercept. Models for daily pollutant data (CO, NO_2, O_3, $PM_{2.5}$, PM_{10}, and SO_2) were adjusted for migration (WCM and ICM), meteorological factors (temperature, accumulated precipitation, wind speed, range of atmospheric pressure, and sunshine duration), and weekend effect (weekend and weekday), incorporating city subclass as the random effect. Significant codes: ***: p-value < 0.001; **: p-value < 0.01; *: p-value < 0.05.

Table 5
Summary of modification effects of city attributes on the migration-pollution relationship.

Modification effect	CO	NO_2	O_3	PM_{10}	$PM_{2.5}$	SO_2
Correlation of ICM	+	+	−	○	+	+
Correlation of WCM	○	+	−	+	+	○
Modification by air pollution						
on ICM	○	↑↑	↓	↓	↓	↓
on WCM	○	↑↑	↑	↑↑	○	○
Combined modification	○	↑↑	↑↑	↓	↓	↓
Modification by city scale						
on ICM	○	○	○	○	↓	○
on WCM	○	↑↑	○	↓	↓	○
Combined modification	○	↑↑	○	↓	↓	○
Modification by response status						
on ICM	○	↑	○	○	null	○
on WCM	○	↑	○	○	null	○
Combined modification	○	↑↑	○	↑	↑	↑

Note: + and − denote the positive and negative coefficients, respectively, in each regression of ln(ICM) and ln(WCM). ↑↑/↑ denotes the strengthening effect of city attributes (increasing trend of positive coefficients or decreasing trend of negative coefficients). ↓/↓↓ denotes the weakening of city attributes (increasing trend of negative coefficients or decreasing trend of increasing coefficients). A double arrow indicates a more significant modification effect. The single arrow indicates slighter but acceptable modification effects, due to the insignificant coefficients not ($p > 0.05$) or the non-monotonic trend. ○ denotes null significant coefficients or modification effects.

NO_2 was slightly stronger in cities with stricter restrictions (intra, 0.3852 μg/m^3; complete, 0.3801 μg/m^3) versus no lockdown (0.3096 μg/m^3).

The effect of the 10% change in ICM on $PM_{2.5}$ was weaker in cities that enforced stricter lockdowns (intra, 0.1976 μg/m^3; complete, 0.2748 μg/m^3) versus no lockdowns (no, 0.4104 μg/m^3; medium, 0.8775 μg/m^3). A null modification of different response statuses was found in the WCM-$PM_{2.5}$ relationship. The response status was not found to modify the effect of migration (WCM and ICM) on PM_{10}, O_3, SO_2, and CO.

The lockdown was associated with air quality improvement. However, stricter lockdowns had a greater impact on air pollution reduction than district lockdowns. Taking NO_2 and $PM_{2.5}$ as an example, ln(ICM) exerted the largest impact on inter-city lockdown cities, followed by complete lockdown, and within-city lockdown cities. Similarly, ln (WCM) had the largest impact on within-city lockdown cities, followed by the complete lockdown and inter-city lockdown cities.

4. Discussion

Air quality improvement is an indirect environmental benefit of lockdown policies in response to the pandemic (Braga et al., 2020; Depellegrin et al., 2020; Wang and Su, 2020; Zeng and Bao, 2021). An annual peak period of returning home and returning to workplaces normally emerges after the Spring Festival holiday. The observed decrease in population migration has been attributed to the pandemic outbreaks and traffic restriction policies (Lau et al., 2021). Nonetheless, cities are inherently heterogeneous entities (Zeng and Bao, 2021). Our study found that the classification of city scale, pollution level, and population mobility is consistent with the characteristics of the cluster mappers of the local Moran's I. This distribution characteristic of the population, economy, urban processes, topography, and climate are consistent in China (H. Wang et al., 2021a). Large urban agglomerations (e.g., the Yangtze River Delta, the Sichuan Basin, the Great Bay area, and Jing-Jin-Ji Region) are densely populated, resulting in serious anthropogenic pollution. Different development levels and pollution conditions, and different lockdown measures in various cities in China during COVID-19 have resulted in complex characteristics of pollution changes. Besides, air pollution has caused a considerable social health burden, and improvements in environmental quality during the COVID-19 could have huge potential health benefits (He et al., 2020). Thus, for public health and city-specific measures to the precise control of complex air pollution, the attributes-specific modification effect (based on natural experimental scenarios during the COVID-19 pandemic) should be studied.

Generally, our research suggests that CO, NO_2, PM_{10}, $PM_{2.5}$, and SO_2 were positively correlated with WCM and ICM, with a negative association between O_3 and migration. This finding has previously been identified in previous studies (Adhikari and Yin, 2020; Bao and Zhang, 2020; Fang et al., 2020; Fronza et al., 2020). The improvements in air quality (despite increases in O_3) caused by the temporary migration reductions were also verified by the weekend effects (Braga et al., 2020). This study determined that the 7-day cycle persisted even during the study period, with serrated grooves on the migration curve. Another study supported our findings on PM emissions in Nice, Rome, and Turin (Sicard et al., 2020). Similarly, a counter-weekend effect on ozone showed that the average O_3 concentration on non-workdays was higher than that on workdays (Wang et al., 2020).

Our results showed that substantial NO_2 reduction appeared in more air-polluted and population-dense cities, or those that applied stringent COVID-19 measures. Transportation is the primary source of NO_2 in China. Megacities and large cities serve as transportation hubs and industry centers more than medium and small cities (Krecl et al., 2020; Lu et al., 2021). Daily commuting, which causes more air pollutants, was much greater than in smaller cities because of the separation of work and residence. Thus, traffic restrictions would directly lead to a reduction in fuel combustion and nitrogen oxide emissions from trains, cars, and airplanes (Kanniah et al., 2020; Kotnala et al., 2020). Another study that examined the effect of vehicle density on air pollution among cities showed that every doubling in vehicle density was in line with a 1.5 μg/m^3 decrease in NO_2 (Jia et al., 2021). This study supports our findings, with a clear linear relationship between vehicle density and a reduction in NO_2 during the traffic control period.

The association between migration and $PM_{2.5}$ and PM_{10} was distinct in small and clean cities. Our result shows that, even at low pollution concentration, small and clean cities can gain more environmental benefits from a proportionate decrease (e.g. 10%) in migration than those in polluted and large cities. Other studies supported our findings, wherein the correlations between migration and air pollution were approximately four to five times greater in more polluted cities than in cleaner cities (He et al., 2020; Mandal and Pal, 2020). Pollution concentrations in regions with more emission sources, such as north-central China, showed a greater rebound than that of surrounding regions (Bao and Zhang, 2020). As polluted and large cities hold more vehicle density and population migration, our results are consistent with other studies that showed vehicle population and urban greening as effect modifiers, wherein the linear association in cities' vehicle density at high levels (exceeded 50/km^2) slightly attenuated for $PM_{2.5}$ and PM_{10} (Jia et al., 2021). Another study provided evidence for the hypothesis that controlling population flow could quickly cause a large marginal effect quickly in cities with high background pollutant concentrations (Leung and Sun, 2020).

Furthermore, the relationship between migration and CO and SO_2 was not sensitive to city size, pollution level, and response status. Existing research findings are inconsistent. Some reported reversed relationship between vehicle density and SO_2 when vehicle density was high (Jia et al., 2021). However, a study found cities with fewer industrial firms witnessed SO2 increase, while cities with more industrial firms recorded a greater reduction (Zeng and Bao, 2021). Although findings from an earlier study provided conflicting evidence of a strengthened modification effect from vehicle density for CO, this study reported no significant association between truck proportion and CO (Jia et al., 2021). They also found no modification effect between vehicle density and SO_2 or O_3 with a two-category division (Jia et al., 2021). Consequently, further studies are warranted to validate our

findings of the modification effect on CO and SO2.

This study observed that response status produced the strongest combined effect modifications of WCM and ICM among these three city attributes. This may be because the response status to COVID-19 was an active action, whereas city scale and air pollution levels were both passive actions. This suggests that city managers have the potential to proactively control air pollution. In addition, the interactions between migration and air pollution may be strengthened by stricter measurements in response to COVID-19, and population migration is known to be closely associated with traffic regulation (Srivastava et al., 2020). Another study that examined the effect of lockdowns and decreases in air pollution concluded that more stringent traffic control measures lead to greater reductions in AQI, $PM_{2.5}$, PM_{10}, NO_2, and CO levels (Jia et al., 2021). Even in a city without a formal lockdown policy, the air quality level decreased. Our results are supported by another study that claimed that disease preventive measures (e.g. the holiday extension, home quarantine, and social distancing policy) may affect no-lockdown cities (He et al., 2020).

The study included 332 Chinese cities, from January to March in 2019, 2020, and 2021, and the results of this study may be generalizable to other regions. Contrasts exist both between and within groups or stratifications of cities; therefore, a linear mixed model with a random subclass-specific intercept was applied in this study. Therefore, the risk of bias due to confounding factors should be dismissed more than those observed in a cross-sectional study design, although bias due to unmeasured or residual confounding can never be eliminated (Regencia et al., 2020). The large-sample analysis further helps to address challenges from city-specific time-invariant characteristics and plausibly estimate the average effect in each subclass of city attributes (He et al., 2020). The novelty of this study is that it identifies the modifier role of city scale, pollution level, and response status in the relationship between migration and air pollution. The evidence from this study may support city-specific air pollution control. Our findings also suggest that initiatives by city managers and residents to reduce emissions can effectively reduce air pollution, even at a relatively low level.

5. Conclusions

In summary, this study documented the modifier role of pollution levels, city size, and response status in the association between air pollution and migration, meteorological data, and weekend effects from January to March (2019–2021) during the COVID-19 period. This study found that in more air-polluted and population-dense, or in those that applied stringent COVID-19 measures, low migration resulted in decreased NO_2 and increased O_3 levels. Cities that are less air-polluted and low-density may benefit more from decreasing PM_{10} and $PM_{2.5}$. Stringent traffic restrictions in response to COVID-19 resulted in stronger environmental improvements than the absence of lockdowns. The relationships between migration and CO and SO_2 were not relatively sensitive to city size, pollution level, or response status. Therefore, the possible modifiers of the relationship between air pollution and CO and SO_2 should be assessed in future studies. In addition, a significant difference was not observed between the modification effect of ICM and WCM on air pollution by city attributes.

Traffic restrictions caused a differential improvement effect in air pollution, regardless of the pollution type or city. The environmental implication of this study is that city-specific government policies should be implemented in the target setting and process path. More polluted cities may gain more marginal environmental benefits from restricting low-level emissions from within-city trips than from restricting inter-city trips. For example, control of emissions from traffic sources is effective in reducing NO_2 pollution, particularly at high pollution levels. Environmentally friendly policies, such as clean-energy vehicles, green commuting and cycling days, and stringent vehicle emission standards, should be supported in NO_2-polluted cities. However, in cities with CO and SO_2 as the primary pollutants, controlling emissions from traffic sources is insufficient to solve this problem. Attention should also be paid to the aggravation of O_3 pollution and to coordinate emission reduction. Generally, periodic initiatives in cities may purposefully reduce pollutant concentrations and improve the self-regulation ability of the social ecosystem. Future environmental policies should pursue similar air quality improvements at a considerably lower economic cost.

This study had certain limitations. The migrations involved in the Baidu migration data were dependent on the availability of smartphones. This may have influenced certain of the findings, for example, the differences between rural areas and mega-cities. In addition, other multiple air pollution sources, such as natural, industrial, and residential sources, may have biased the result, although emissions from other sources may have contributed to air pollution, they remained at a stable level during the implementation of traffic control.

Author contributions

Keyu Luo: Methodology, Software, Writing - Original Draft and Editing, Visualization; Zhenyu Wang: Conceptualization, Writing - Review and Editing, Supervision; Jiansheng Wu: Resources, Funding acquisition, Project administration.

Funding

This work was supported by the Shenzhen Fundamental Research Program (No. GXWD20201231165807007-20200816003026001) and China Postdoctoral Science Foundation (2020M680248).

Declaration of competing interest

The authors declare that they have no known competing financial interests or personal relationships that could have appeared to influence the work reported in this paper.

Appendix A. Supplementary data

Supplementary data to this article can be found online at https://doi.org/10.1016/j.apr.2022.101419.

References

Adhikari, A., Yin, J., 2020. Short-term effects of Ambient Ozone, PM2.5, and meteorological factors on COVID-19 confirmed cases and deaths in Queens, New York. Int. J. Environ. Res. Publ. Health 17, 1–13. https://doi.org/10.3390/ijerph17114047.

Aunan, K., Hansen, M.H., Wang, S., 2018. Introduction: air pollution in China. China Q. 234, 279–298. https://doi.org/10.1017/S0305741017001369.

Bao, R., Zhang, A., 2020. Does lockdown reduce air pollution? Evidence from 44 cities in northern China. Sci. Total Environ. 731 https://doi.org/10.1016/j.scitotenv.2020.139052.

Bashir, M.F., Ma, B., Bilal Komal, B., Bashir, M.A., Tan, D., Bashir, M., 2020. Correlation between climate indicators and COVID-19 pandemic in New York, USA. Sci. Total Environ. 728, 138835. https://doi.org/10.1016/j.scitotenv.2020.138835.

Bherwani, H., Nair, M., Musugu, K., Gautam, S., Gupta, A., Kapley, A., Kumar, R., 2020. Valuation of air pollution externalities: comparative assessment of economic damage and emission reduction under COVID-19 lockdown. Air Qual. Atmos. Heal. 13, 683–694. https://doi.org/10.1007/s11869-020-00845-3.

Braga, F., Scarpa, G.M., Brando, V.E., Manfè, G., Zaggia, L., 2020. COVID-19 lockdown measures reveal human impact on water transparency in the Venice Lagoon. Sci. Total Environ. 736 https://doi.org/10.1016/j.scitotenv.2020.139612.

Chen, Y., Jin, G.Z., Kumar, N., Shi, G., 2013. The promise of Beijing: evaluating the impact of the 2008 Olympic Games on air quality. J. Environ. Econ. Manag. 66, 424–443. https://doi.org/10.1016/j.jeem.2013.06.005.

Chen, K., Wolf, K., Breitner, S., Gasparrini, A., Stafoggia, M., Samoli, E., Andersen, Z.J., Bero-Bedada, G., Bellander, T., Hennig, F., Jacquemin, B., Pekkanen, J., Hampel, R., Cyrys, J., Peters, A., Schneider, A., 2018. Two-way effect modifications of air pollution and air temperature on total natural and cardiovascular mortality in eight European urban areas. Environ. Int. 116, 186–196. https://doi.org/10.1016/j.envint.2018.04.021.

Chen, H., Chen, Y., Lian, Z., Wen, L., Sun, B., Wang, P., Li, X., Liu, Q., Yu, X., Lu, Y., Qi, Y., Zhao, S., Zhang, L., Yi, X., Liu, F., Pan, G., 2020a. Correlation between the migration scale index and the number of new confirmed coronavirus disease 2019 cases in China. Epidemiol. Infect. https://doi.org/10.1017/S0950268820001119.

Chen, X., Li, F., Zhang, J., Zhou, W., Wang, X., Fu, H., 2020b. Spatiotemporal mapping and multiple driving forces identifying of PM2.5 variation and its joint management strategies across China. J. Clean. Prod. 250, 119534. https://doi.org/10.1016/j.jclepro.2019.119534.

Depellegrin, D., Bastianini, M., Fadini, A., Menegon, S., 2020. The effects of COVID-19 induced lockdown measures on maritime settings of a coastal region. Sci. Total Environ. 740, 140123. https://doi.org/10.1016/j.scitotenv.2020.140123.

Fang, K., Wang, Tingting, He, J., Wang, Tijian, Xie, X., Tang, Y., Shen, Y., Xu, A., 2020. The distribution and drivers of PM2.5 in a rapidly urbanizing region: the Belt and Road Initiative in focus. Sci. Total Environ. 716, 137010. https://doi.org/10.1016/j.scitotenv.2020.137010.

Faridi, S., Yousefian, F., Janjani, H., Niazi, S., Azimi, F., Naddafi, K., Hassanvand, M.S., 2021. The effect of COVID-19 pandemic on human mobility and ambient air quality around the world: a systematic review. Urban Clim. 38, 100888. https://doi.org/10.1016/j.uclim.2021.100888.

Fronza, R., Lusic, M., Schmidt, M., Lucic, B., 2020. Spatial–temporal variations in atmospheric factors contribute to SARS-CoV-2 outbreak. Viruses 12. https://doi.org/10.3390/v12060588.

Gautam, S., 2020. COVID-19: air pollution remains low as people stay at home. Air Qual. Atmos. Heal. 13, 853–857. https://doi.org/10.1007/s11869-020-00842-6.

Gibbs, H., Liu, Y., Pearson, C.A.B., Jarvis, C.I., Grundy, C., Quilty, B.J., Diamond, C., Simons, D., Gimma, A., Leclerc, Q.J., Auzenbergs, M., Lowe, R., O'Reilly, K., Quaife, M., Hellewell, J., Knight, G.M., Jombart, T., Klepac, P., Procter, S.R., Deol, A. K., Rees, E.M., Flasche, S., Kucharski, A.J., Abbott, S., Sun, F.Y., Endo, A., Medley, G., Munday, J.D., Meakin, S.R., Bosse, N.I., Edmunds, W.J., Davies, N.G., Prem, K., Hué, S., Villabona-Arenas, C.J., Nightingale, E.S., Houben, R.M.G.J., Foss, A.M., Tully, D.C., Emery, J.C., van Zandvoort, K., Atkins, K.E., Rosello, A., Funk, S., Jit, M., Clifford, S., Russell, T.W., Eggo, R.M., 2020. Changing travel patterns in China during the early stages of the COVID-19 pandemic. Nat. Commun. 11 https://doi.org/10.1038/s41467-020-18783-0.

Guo, H., Wei, J., Li, X., Ho, H.C., Song, Y., Wu, J., Li, W., 2021. Do socioeconomic factors modify the effects of PM1 and SO2 on lung cancer incidence in China? Sci. Total Environ 756, 143998. https://doi.org/10.1016/j.scitotenv.2020.143998.

Han, L., Zhou, W., Li, W., Qian, Y., 2017. Global population exposed to fine particulate pollution by population increase and pollution expansion. Air Qual. Atmos. Heal. 10, 1221–1226. https://doi.org/10.1007/s11869-017-0506-8.

He, C., Hong, S., Zhang, L., Mu, H., Xin, A., Zhou, Y., Liu, J., Liu, N., Su, Y., Tian, Y., Ke, B., Wang, Y., Yang, L., 2021a. Global, continental, and national variation in PM2.5, O3, and NO2 concentrations during the early 2020 COVID-19 lockdown. Atmos. Pollut. Res. 12, 136–145. https://doi.org/10.1016/j.apr.2021.02.002.

He, C., Yang, L., Cai, B., Ruan, Q., Hong, S., Wang, Z., 2021b. Impacts of the COVID-19 event on the NOx emissions of key polluting enterprises in China. Appl. Energy 281, 116042. https://doi.org/10.1016/j.apenergy.2020.116042.

He, G., Pan, Y., Tanaka, T., 2020. The short-term impacts of COVID-19 lockdown on urban air pollution in China. Nat. Sustain. 3, 1005–1011. https://doi.org/10.1038/s41893-020-0581-y.

Hu, M., Chen, Z., Cui, H., Wang, T., Zhang, C., Yun, K., 2021. Air pollution and critical air pollutant assessment during and after COVID-19 lockdowns: evidence from pandemic hotspots in China, the Republic of Korea, Japan, and India. Atmos. Pollut. Res. 12, 316–329. https://doi.org/10.1016/j.apr.2020.11.013.

Jia, C., Li, W., Wu, T., He, M., 2021. Road traffic and air pollution: evidence from a nationwide traffic control during coronavirus disease 2019 outbreak. Sci. Total Environ. 781, 146618. https://doi.org/10.1016/j.scitotenv.2021.146618.

Kanniah, K.D., Kamarul Zaman, N.A.F., Kaskaoutis, D.G., Latif, M.T., 2020. COVID-19's impact on the atmospheric environment in the Southeast Asia region. Sci. Total Environ. 736, 139658. https://doi.org/10.1016/j.scitotenv.2020.139658.

Kerimray, A., Baimatova, N., Ibragimova, O.P., Bukenov, B., Kenessov, B., Plotitsyn, P., Karaca, F., 2020. Assessing air quality changes in large cities during COVID-19 lockdowns: the impacts of traffic-free urban conditions in Almaty. Kazakhstan. Sci. Total Environ. 730 https://doi.org/10.1016/j.scitotenv.2020.139179.

Kotnala, G., Mandal, T.K., Sharma, S.K., Kotnala, R.K., 2020. Emergence of blue Sky over Delhi due to coronavirus disease (COVID-19) lockdown implications. Aerosol Sci. Eng. 4, 228–238. https://doi.org/10.1007/s41810-020-00062-6.

Krecl, P., Targino, A.C., Oukawa, G.Y., Cassino Junior, R.P., 2020. Drop in urban air pollution from COVID-19 pandemic: policy implications for the megacity of São Paulo. Environ. Pollut. 265, 19–21. https://doi.org/10.1016/j.envpol.2020.114883.

Lau, H., Khosrawipour, V., Kocbach, P., Mikolajczyk, A., Schubert, J., Bania, J., Khosrawipour, T., 2021. The positive impact of lockdown in Wuhan on containing the COVID-19 outbreak in China. J. Trav. Med. 27, 1–7. https://doi.org/10.1093/JTM/TAAA037.

Leung, W.W.F., Sun, Q., 2020. Electrostatic charged nanofiber filter for filtering airborne novel coronavirus (COVID-19) and nano-aerosols. Separ. Purif. Technol. 250, 116886. https://doi.org/10.1016/j.seppur.2020.116886.

Liu, J., Zhou, J., Yao, J., Zhang, X., Li, L., Xu, X., He, X., Wang, B., Fu, S., Niu, T., Yan, J., Shi, Y., Ren, X., Niu, J., Zhu, W., Li, S., Luo, B., Zhang, K., 2020. Impact of meteorological factors on the COVID-19 transmission: a multi-city study in China. Sci. Total Environ. 726, 138513. https://doi.org/10.1016/j.scitotenv.2020.138513.

Lu, D., Zhang, J., Xue, C., Zuo, P., Chen, Z., Zhang, L., Ling, W., Liu, Q., Jiang, G., 2021. COVID-19-Induced lockdowns indicate the short-term control effect of air pollutant emission in 174 cities in China. Environ. Sci. Technol. 55, 4094–4102. https://doi.org/10.1021/acs.est.0c07170.

Mandal, I., Pal, S., 2020. COVID-19 pandemic persuaded lockdown effects on environment over stone quarrying and crushing areas. Sci. Total Environ. 732, 139281. https://doi.org/10.1016/j.scitotenv.2020.139281.

Naqvi, H.R., Mutreja, G., Hashim, M., Singh, A., Nawazuzzoha, M., Naqvi, D.F., Siddiqui, M.A., Shakeel, A., Chaudhary, A.A., Naqvi, A.R., 2021. Global assessment of tropospheric and ground air pollutants and its correlation with COVID-19. Atmos. Pollut. Res. 12, 101172. https://doi.org/10.1016/j.apr.2021.101172.

Regencia, Z.J.G., Dalmacion, G.V., Quizon, D.B., Quizon, K.B., Duarte, N.E.P., Baja, E.S., 2020. Airborne heavy metals and blood pressure: modification by sex and obesity in the MMDA traffic enforcers' health study. Atmos. Pollut. Res. 11, 2244–2250. https://doi.org/10.1016/j.apr.2020.06.015.

Rugani, B., Caro, D., 2020. Impact of COVID-19 outbreak measures of lockdown on the Italian Carbon Footprint. Sci. Total Environ. 737, 139806. https://doi.org/10.1016/j.scitotenv.2020.139806.

Sharma, S., Zhang, M., Anshika Gao, J., Zhang, H., Kota, S.H., 2020. Effect of restricted emissions during COVID-19 on air quality in India. Sci. Total Environ. 728 https://doi.org/10.1016/j.scitotenv.2020.138878.

Shen, L., Wang, H., Zhu, B., Zhao, T., Liu, A., Lu, W., Kang, H., Wang, Y., 2021. Impact of urbanization on air quality in the Yangtze River Delta during the COVID-19 lockdown in China. J. Clean. Prod. 296, 126561. https://doi.org/10.1016/j.jclepro.2021.126561.

Sicard, P., De Marco, A., Agathokleous, E., Feng, Z., Xu, X., Paoletti, E., Rodriguez, J.J.D., Calatayud, V., 2020. Amplified ozone pollution in cities during the COVID-19 lockdown. Sci. Total Environ. 735, 139542. https://doi.org/10.1016/j.scitotenv.2020.139542.

Srivastava, S., Kumar, A., Bauddh, K., Gautam, A.S., Kumar, S., 2020. 21-Day lockdown in India dramatically reduced air pollution indices in Lucknow and New Delhi, India. Bull. Environ. Contam. Toxicol. 105, 9–17. https://doi.org/10.1007/s00128-020-02895-w.

Wang, H., Zhao, L., Xie, Y., Hu, Q., 2016. APEC blue"-The effects and implications of joint pollution prevention and control program. Sci. Total Environ. 553, 429–438. https://doi.org/10.1016/j.scitotenv.2016.02.122.

Wang, H., Tan, Y., Zhang, L., Shen, L., Zhao, T., Dai, Q., Guan, T., Ke, Y., Li, X., 2021a. Characteristics of air quality in different climatic zones of China during the COVID-19 lockdown. Atmos. Pollut. Res. 12, 101247. https://doi.org/10.1016/j.apr.2021.101247.

Wang, Z., Li, J., Liang, L., 2020. Spatio-temporal evolution of ozone pollution and its influencing factors in the Beijing-Tianjin-Hebei Urban Agglomeration. Environ. Pollut. 256, 113419. https://doi.org/10.1016/j.envpol.2019.113419.

Wang, Q., Su, M., 2020. A preliminary assessment of the impact of COVID-19 on environment – a case study of China. Sci. Total Environ. 728, 138915. https://doi.org/10.1016/j.scitotenv.2020.138915.

Wang, J., Xu, X., Wang, S., He, S., Li, X., He, P., 2021b. Heterogeneous effects of COVID-19 lockdown measures on air quality in Northern China. Appl. Energy 282, 116179. https://doi.org/10.1016/j.apenergy.2020.116179.

Wang, Y., Yuan, Y., Wang, Q., Liu, C.G., Zhi, Q., Cao, J., 2020. Changes in air quality related to the control of coronavirus in China: implications for traffic and industrial emissions. Sci. Total Environ. 731, 139133. https://doi.org/10.1016/j.scitotenv.2020.139133.

Xiong, Y., Wang, Y., Chen, F., Zhu, M., 2020. Spatial statistics and influencing factors of the COVID-19 epidemic at both prefecture and county levels in Hubei Province, China. Int. J. Environ. Res. Publ. Health 17. https://doi.org/10.3390/ijerph17113903.

Xu, X., Zhang, T., 2020. Spatial-temporal variability of PM2.5 air quality in Beijing, China during 2013–2018. J. Environ. Manag. 262 https://doi.org/10.1016/j.jenvman.2020.110263.

Zeng, J., Bao, R., 2021. The impacts of human migration and city lockdowns on specific air pollutants during the COVID-19 outbreak: a spatial perspective. J. Environ. Manag. 282, 111907. https://doi.org/10.1016/j.jenvman.2020.111907.

Zhang, Q., Zheng, Y., Tong, D., Shao, M., Wang, S., Zhang, Y., Xu, X., Wang, J., He, H., Liu, W., Ding, Y., Lei, Y., Li, J., Wang, Z., Zhang, X., Wang, Y., Cheng, J., Liu, Y., Shi, Q., Yan, L., Geng, G., Hong, C., Li, M., Liu, F., Zheng, B., Cao, J., Ding, A., Gao, J., Fu, Q., Huo, J., Liu, B., Liu, Z., Yang, F., He, K., Hao, J., 2019. Drivers of improved PM2.5 air quality in China from 2013 to 2017. Proc. Natl. Acad. Sci. U. S. A 116, 24463–24469. https://doi.org/10.1073/pnas.1907956116.

Zhang, W., Wang, H., Zhang, X., Peng, Y., Zhong, J., Wang, Y., Zhao, Y., 2020. Evaluating the contributions of changed meteorological conditions and emission to substantial reductions of PM2.5 concentration from winter 2016 to 2017 in Central and Eastern China. Sci. Total Environ. 716, 136892. https://doi.org/10.1016/j.scitotenv.2020.136892.

Zhao, Z., Zhou, Z., Russo, A., Xi, H., Zhang, J., Du, H., Zhou, C., 2021. Comparative analysis of the impact of weather conditions and human activities on air quality in the Dongting and Poyang Lake Region during the COVID-19 pandemic. Atmos. Pollut. Res. 12, 101054. https://doi.org/10.1016/j.apr.2021.101054.